Available online at www.sciencedirect.com
ScienceDirect
Polyhedron 26 (2007) 589–599
POLYHEDRON
www.elsevier.com/locate/poly

Electrostatic forces that determine O,O-*trans* versus O,S-*cis* conformers in the aminated porphyrin complexes of Cd(N-NHCO-2-C_4H_3O-tpp)(OAc) and Cd(N-NHCO-2-C_4H_3S-tpp)(OAc)

Jo-Yu Tung [a,*], Jyh-Horung Chen [b]

[a] *Department of Occupational Safety and Health, Chung Hwai College of Medical Technology, Tainan 713, Taiwan*
[b] *Department of Chemistry, National Chung Hsing University, Taichung 40227, Taiwan*

Received 8 June 2006; accepted 14 August 2006
Available online 19 September 2006

Abstract

Two new diamagnetic, mononuclear and aminated porphyrin complexes of O,O-*trans*-Cd (**3**-*trans*) and O,S-*cis*-Cd (**4**-*cis*) have been synthesized and characterized by ^1H, ^{13}C NMR spectroscopy. The crystal structures of (acetato)(N-2-furancarboxamido-*meso*-tetraphenylporphyrinato)cadmium(II) [Cd(N-NHCO-2-C_4H_3O-tpp)(OAc); **3**-*trans*] and (acetato)(N-2-thiophenecarboxamido-*meso*-tetraphenylporphyrinato)cadmium(II) [Cd(N-NHCO-2-C_4H_3S-tpp)(OAc); **4**-*cis*] were determined. The coordination sphere around Cd^{2+} is a distorted square-based pyramid in which the apical site is occupied by a bidentate chelating OAc^- group for **3**-*trans* and **4**-*cis*. The plane of three pyrrole nitrogen atoms [i.e., N(1), N(2), N(4) for **3**-*trans* and N(1), N(2), N(3) for **4**-*cis*] strongly bonded to Cd^{2+} is adopted as a reference plane 3N. The N(3) and N(4) pyrrole rings bearing the 2-furancarboxamido (Fr) and 2-thiophenecarboxamido groups in **3**-*trans* and **4**-*cis*, respectively, deviate mostly from the 3N plane, thus orienting separately with a dihedral angle of 33.4° and of 31.0°. In **3**-*trans*, Cd^{2+} and N(5) are located on different sides at 1.06 and −1.49 Å from its 3N plane, while in **4**-*cis*, Cd^{2+} and N(5) are also located on different sides at 1.04 and −1.53 Å from its 3N plane. An attractive electrostatic interaction between the Cd^{2+} and $O(4)^-$ atoms in furan stabilizes the O,O-*trans* conformer of **3**. A repulsive electrostatic interaction between Cd^{2+} and $S(1)^+$ destabilizes the O,S-*trans* conformer of **4**. Both of these repulsive and the mutually attractive interactions between $S(1)^+$ and $O(3)^-$ atoms favor the O,S-*cis* rotamer of **4** both in the vapor phase and in low polarity solvents. NOE difference spectroscopy, HMQC and HMBC were employed for the unambiguous assignment of the ^1H and ^{13}C NMR resonances of **3**-*trans* and **4**-*cis* in $CDCl_3$ at 20 and −50 °C.

Keywords: Cadmium; X-ray diffraction; Electrostatic interaction; O,O-*trans*; O,S-*cis* conformer

1. Introduction

There have been numerous investigations on the rotational equilibrium between the two *anti* and *syn* planar isomers of 2-acyl-furans and -thiophenes (i.e., R = H, CH_3, Et, Pr^i, pentan-3-yl, Bu^t, Cl, F, Bu^tO) [1–6]

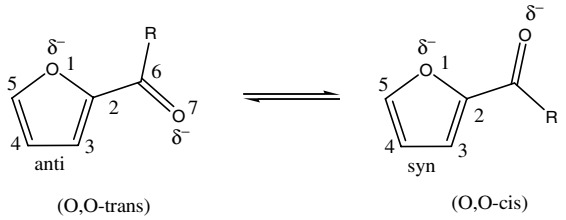

(1)

* Corresponding author. Tel.: +886 6 2674567x815; fax: +886 6 2894028.
E-mail address: joyuting@mail.hwai.edu.tw (J.-Y. Tung).

0277-5387/$ - see front matter © 2006 Published by Elsevier Ltd.
doi:10.1016/j.poly.2006.08.034

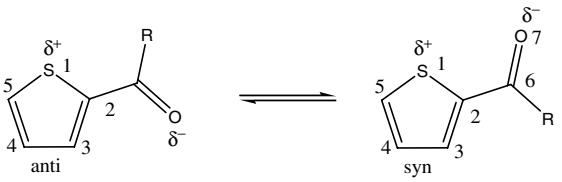

(O,S-trans) (O,S-cis) (2)

Group charge density calculations reveal that both oxygen atoms in 2-acyl-furans of the *syn* form, being strongly charged, face increasing repulsive electrostatic interactions (see Eq. (1)). However, in the thiophene carbonyl derivatives, the S atom is positively charged and consequently there is an attractive electrostatic interaction between the S and O atoms in *cis* form (see Eq. (2)) [1]. The major factor determining the stability or instability of the *cis*-isomer is a repulsive electrostatic interaction between the two oxygen atoms for furan carbonyl and an attractive electrostatic interaction between the sulfur and oxygen atoms for the thiophene carbonyl. The O,O-*trans* form has a relatively low dipole moment and is favored in the gas phase or in low polar solvents with dielectric constants (ε) smaller than 5. In a more polar medium, the O,O-*cis* isomer with a higher dipole moment (μ) is favored due to a stronger solute–solvent interaction; as a result the O,O-*cis* form in 2-acyl-furans can be more stable than the O,O-*trans* isomer in solution when the energy difference ΔE ($= E_{syn} - E_{anti}$) is relatively small and $\Delta\mu$ ($= \mu_{syn} - \mu_{anti}$) is large in the gas phase. In the case of the thiophene-2-carbonyl derivative, the more polar O,S-*cis* conformation is found to be more stable in the vapor phase; the *cis* form also predominates in solutions of different polarity; the amount of O,S-*cis* isomer increases slightly with solvent polarity. The energy differences (ΔE) between the rotamers are 4–13 kJ/mol, but the barrier to rotation is ca. 42 kJ/mol [1].

The preparation of *N*-substituted-*N*-aminoporphyrin has been described by three groups [7–11]. In *N*-substituted-*N*-aminoporphyrin, when the H atom of NH_2 is replaced either by the 2-furoncarboxyamino ligand or by the 2-thiophenecarboxyamino group, two new free aminated porphyrins are formed, namely N-2-furancarboxamido-*meso*-tetraphenylporphyrin (N-NHCO-2-C_4H_3-OHtpp; **1**) and N-2-thiophenecarboxamido-*meso*-tetraphenylporphyrin (N-NHCO-2-C_4H_3S-Htpp; **2**) [tpp = dianion of *meso*-tetraphenylporphyrin], which are derivatives of 2-acyl-furans and -thiophenes, respectively. A thorough review of the literature shows that there is no prior report on the metal complexes of **1** and **2**. The lack of previous work on metal complexes of these two ligands prompted us to undertake the synthesis and structural studies of the Cd(II) complexes. Metallation of these aminated porphyrins could lead to mononuclear metal complexes in which the metal is coordinated to four porphyrinic N atoms. Cd(II) is a diamagnetic ion and maintains the d^{10} electron configuration which minimizes intrinsic coordination geometry preferences while favoring coordination by softer ligands. In this paper, we describe the X-ray structural investigation on the metallation of **1** and **2** leading to mononuclear complexes of (acetato)(N-2-furancarboxamido-*meso*-tetraphenylporphyrinato)cadmium(II) [Cd(N-NHCO-2-C_4H_3O-tpp)(OAc); **3**] and (acetato)(N-2-thiophenecarboxamido-*meso*-tetraphenylporphyrinato)cadmium(II) [Cd(N-NHCO-2-C_4H_3S-tpp)(OAc); **4**], respectively. This metallation introduces the metal electrostatic interaction between the Cd(II) atom and the heteroatom of the ring in **3** and **4** as the diamagnetic Cd(II) is just located in the vicinity of the furonylcarboxamido (or thiophenecarboxamido) group in **3** (or **4**). We try to figure out how the metal electrostatic effect influences the O,O-Cd and O,S-Cd conformers of **3** and **4**, respectively. These metal electrostatic effects could be applied to explain the various conformations of thallium(III), bismuth(III) and tin(IV) porphyrin complexes with O,O and O,S rotamers.

2. Experimental

2.1. N-NHCO-2-C_4H_3O-Htpp (1) [9]

A mixture of NaN_3 (1.00 g, 1.54×10^{-2} mol) in distilled water (2 cm^3) and 2-furoyl chloride (2.5 mL, 2.54×10^{-2} mol) was stirred for 30 min. After concentration, the residue was dissolved in CH_2Cl_2 and filtered to remove excess NaN_3 and NaCl. The CH_2Cl_2 layer contained 2-furancarbonyl azide ($C_4H_3OCON_3$). A solution of Zn(tpp) (0.30 g, 1.36×10^{-3} mol) and the above $C_4H_3OCON_3$ in CH_2Cl_2 (100 cm^3) in a stoppered 250 mL Erlenmeyer flask was left for ca. 24 h in the sunlight. To this solution was then added 0.5 N HCl (250 cm^3) with vigorous shaking for 0.5 h. The organic layer, green in color, was separated, solid ammonium carbonate was added to it, and then dried with anhydrous Na_2SO_4. The excess $(NH_4)_2CO_3$ and Na_2SO_4 were removed by filtration. After concentration, the residue was dissolved in a minimum of CH_2Cl_2 and chromatographed on silica gel (50.00 g, 70–230 mesh). The dimensions of the silica gel column were 1.5×17 in. The desired compound was eluted with ethyl acetate (EtOAc)–CH_2Cl_2 [1:9 (v/v)] as a dark purple band on silica gel. Removal of the solvent and recrystallization from CH_2Cl_2–MeOH [1:2 (v/v)] gave the purple solid N-NHCO-2-C_4H_3O-Htpp (**1**) (0.165 g, 2.28×10^{-4} mol, 46.8%), which was again dissolved in CH_2Cl_2 and layered with CH_3OH to get purple crystals for single crystal X-ray analysis. ^{1}H NMR (599.95 MHz, $CDCl_3$, 20 °C): δ 9.12 [d, $H_\beta(10,19)$, ^3J(H–H) = 4.4 Hz], H_β(a,b) represents two equivalent β-pyrrole protons attached to carbons a and b, respectively; 8.90 [d, $H_\beta(9,20)$, ^3J(H–H) = 4.8 Hz]; 8.88 [s, $H_\beta(4,5)$]; 8.35 [bs, *o*′-H(34,44) and *o*′-H(38,40)], where *o*-H = *ortho* protons; 8.28 [d, *o*-H(26,28), ^3J(H–H) = 6.6 Hz]; 8.19 [d, *o*-H(22,32), ^3J(H–H) = 6.6 Hz]; 8.09 [s, $H_\beta(14,15)$]; 7.78–7.82 (m) for *meta* and *para* protons; 5.79 [s, Fr-H_5]; 4.69 [q, Fr-H_4, ^3J(Fr-H_4, Fr-H_5) = 1.8 Hz and ^3J(Fr-H_4, Fr-H_3) = 3.6 Hz]; 1.35 [s, Fr-H_3], where Fr = 2-furancarboxamido. MS (FAB): M^+

724 (calcd for $C_{49}H_{33}N_5O_2$: 724). UV/Vis spectrum, λ (nm) [$\varepsilon \times 10^{-3}$ (M^{-1} cm^{-1})] in CH_2Cl_2: 429 (246.6), 541 (10.2), 582 (10.2), 638 (7.8).

2.2. Preparation of N-NHCO-2-C_4H_3S-Htpp (2) [9]

A mixture of NaN_3 (1.00 g, 1.54×10^{-2} mol) in distilled water (2 cm^3) and 2-thiophenecarbonylchloride (2.5 mL) was stirred for 20 min. After concentration, the residue was dissolved in CH_2Cl_2 and filtered to remove excess NaN_3 and NaCl. The CH_2Cl_2 layer contains 2-thiophenecarbonyl azide ($C_4H_3SCON_3$). A solution of Zn(tpp) (0.27 g, 3.04×10^{-4} mol) and the above $C_4H_3SCON_3$ in CH_2Cl_2 (200 cm^3) in a stoppered 250 mL Erlenmeyer flask was left for ca. 8 h in the sunlight. To this solution was then added 0.5 N HCl (250 cm^3) with vigorous shaking for 0.5 h. The organic layer was separated, solid ammonium carbonate added to it, and then dried with anhydrous Na_2SO_4. The excess $(NH_4)_2CO_3$ and Na_2SO_4 were removed by filtration. After concentration, the residue was dissolved in a minimum of CH_2Cl_2 and chromatographed on silica gel (100.00 g, 70–230 mesh). The dimensions of the silica gel column were 1.5×17 in. The desired compound was eluted with ethyl acetate (EtOAc)–CH_2Cl_2 [1:4 (v/v)] as a dark brown band on silica gel. Removal of the solvent and recrystallization from CH_2Cl_2–MeOH [1:2 (v/v)] gave the purple solid of N-NHCO-2-C_4H_3S-Htpp (**2**) (0.17 g, 2.06×10^{-4} mol, 68%) which was again dissolved in CH_2Cl_2 and layered with CH_3CN to get purple crystals for single crystal X-ray analysis. ^1H NMR (599.95 MHz, $CDCl_3$, 20 °C): δ 9.10 [d, $H_\beta(10,19)$, ^3J(H–H) = 4.2 Hz]; 8.87 [d, $H_\beta(9,20)$, ^3J(H–H) = 4.2 Hz]; 8.85 [s, $H_\beta(4,5)$]; 8.36 [bs, o'-H(34,44) and o'-H(38,40)], where o-H = *ortho* protons; 8.25 [d, o-H(22,32), ^3J(H–H) = 7.2 Hz]; 8.16 [d, o-H(26,28), ^3J(H–H) = 7.2 Hz]; 8.06 [s, $H_\beta(14,15)$]; 7.75–7.80 (m) for *meta* and *para* protons; 5.85 [dd, S-H_5, ^3J(S-H_4, S-H_5) = 5.0 Hz and ^4J(S-H_3, S-H_5) = 1.2 Hz], where S = 2-thiophenecarboxamido; 5.43 [dd, S-H_4, ^3J(S-H_3, S-H_4) = 3.8 Hz and ^3J(S-H_4, S-H_5) = 5.0 Hz]; 3.47 [dd, S-H_3, ^3J(S-H_3, S-H_4) = 3.8 Hz and ^4J(S-H_3, S-H_5) = 1.2 Hz]; −0.35 (s, NH). MS (FAB): M^+ 740 (calcd for $C_{49}H_{33}N_5OS$: 740). UV/Vis spectrum, λ (nm) [$\varepsilon \times 10^{-3}$ (M^{-1} cm^{-1})] in CH_2Cl_2: 430 (278), 541 (21.8), 583 (21.7), 639 (19.4).

2.3. Preparation of Cd(N-NHCO-2-C_4H_3O-tpp)(OAc) (3)

A mixture of N-NHCO-2-C_4H_3O-Htpp (**1**) (76 mg, 0.1 mmol) in CH_2Cl_2 (5 cm^3) and $Cd(OAc)_2 \cdot 2H_2O$ (69 mg, 0.3 mmol) in MeOH (2 cm^3) were refluxed in CH_3CN (20 cm^3) for 3 h. After concentration, the residue was dissolved in CH_2Cl_2 and washed with distilled water to remove excess $Cd(OAc)_2 \cdot 2H_2O$. The CH_2Cl_2 layer was concentrated to dryness affording a blue precipitate, which was recrystallized from toluene–hexane [1:3 (v/v)] yielding a dark blue solid of **3** (51 mg, 0.0548 mmol, 55%). Compound **3** was redissolved in CH_2Cl_2 and layered with toluene to afford blue crystals for single-crystal X-ray analysis. ^1H NMR (599.95 MHz, $CDCl_3$, 20 °C): δ 8.89 [s, $H_\beta(2,3)$]; 8.76 [d, $H_\beta(14,35)$, ^3J(H–H) = 4.5 Hz]; 8.73 [d, $H_\beta(13,36)$, ^3J(H–H) = 4.5 Hz]; 8.61 [s, $H_\beta(24,25)$]; 8.62 [d, o-H(22,29), ^3J(H–H) = 6.6 Hz]; 8.40 [d, o-H(18,33), ^3J(H–H) = 6.6 Hz]; 7.75–7.86 (m, *meta* and *para* protons); 5.72 (s, Fr-H_5); 5.20 (s, Fr-H_4); 4.37 (s, Fr-H_3); 0.17 (s, OAc-Me), −0.99 (s, NH). ^1H NMR (599.95 Hz, $CDCl_3$, −50 °C): δ 8.96 [s, $H_\beta(2,3)$]; 8.76 [d, $H_\beta(14,35)$, ^3J(H–H) = 4.2 Hz]; 8.73 [d, $H_\beta(13,36)$, ^3J(H–H) = 7.8 Hz]; 8.70 [s, $H_\beta(24,25)$]; 8.64 [d, o-H(22,29), ^3J(H–H) = 7.8 Hz]; 8.48 [d, o-H(18,33), ^3J(H–H) = 7.2 Hz]; 8.42 [d, o'-H(11,40), ^3J(H–H) = 4.8 Hz]; 8.20 [d, o'-H(7,44), ^3J(H–H) = 7.2 Hz]; 7.75–7.91 (m, *meta* and *para* protons); 5.74 (s, Fr-H_5); 5.24 [d, Fr-H_4, ^3J(H–H) = 1.8 Hz]; 4.52 (s, Fr-H_3); 0.18 (s, OAc-Me); −1.12 (s, NH). ^{13}C NMR (150.87 MHz, 20 °C, $CDCl_3$): δ 154.0 [s, $C_\alpha(1,4)$]; 153.9 [s, $C_\alpha(15,34)$]; 152.2 [s, $C_\alpha(12,37)$]; 150.2 [s, $C_\alpha(23,26)$]; 134.11 [s, $C_\beta(2,3)$]; 134.06 [s, $C_\beta(13,36)$]; 131.5 [s, $C_\beta(14,35)$]; 123.9 [s, $C_\beta(24,25)$]; 121.9 [s, $C_m(16,17)$]; 152.2 [s, Fr–CO]; 141.8 [s, Fr–C_2]; 108.7 [s, Fr–C_3]; 110.2 [s, Fr–C_4]; 143.5 [s, Fr–C_5]; 176.3 [s, OAc-CO]; 18.9 [s, OAc-Me]. MS (FAB): $(M-OAc)^+$ 834 (calcd for $C_{49}H_{31}CdN_5O_2$: 834). UV/Vis spectrum, λ (nm) [$\varepsilon \times 10^{-3}$ (M^{-1} cm^{-1})] in CH_2Cl_2: 442.0 (233.1), 619.1 (17).

2.4. Preparation of Cd(N-NHCO-2-C_4H_3S-tpp)(OAc) (4)

Compound **4** was prepared in the same way as described for **3** in a 52% yield using N-NHCO-2-C_4H_3S-Htpp (**2**). Compound **4** was dissolved in CH_2Cl_2 and layered with toluene to obtain blue crystals for single-crystal X-ray analysis. ^1H NMR (599.95 MHz, $CDCl_3$, 20 °C):δ 8.89 [s, $H_\beta(4,5)$]; 8.76 [d, $H_\beta(10,19)$, ^3J(H–H) = 4.2 Hz]; 8.72 [d, $H_\beta(9,20)$, ^3J(H–H) = 4.2 Hz]; 8.63 [s, $H_\beta(14,15)$]; 8.60 [d, o-H(38,40), ^3J(H–H) = 7.2 Hz]; 8.40 [d, o-H(34,44), ^3J(H–H) = 6.6 Hz]; 7.74–7.86 (m, *meta* and *para* protons); 6.34 [d, S-H_5, ^3J(H–H) = 4.8 Hz]; 5.57 [t, S-H_4, ^3J(H–H) = 4.2 Hz]; 2.99 [d, S-H_3, ^3J(H–H) = 3 Hz]; 0.15 (s, OAc-Me), −1.23 (s, NH). ^1H NMR (599.95 MHz, $CDCl_3$, −50 °C): δ 8.95 [s, $H_\beta(4,5)$]; 8.75 [d, $H_\beta(10,19)$, ^3J(H–H) = 3.6 Hz]; 8.71 [s, $H_\beta(14,15)$]; 8.70 [d, $H_\beta(9,20)$, ^3J(H–H) = 3.6 Hz]; 8.61 [d, o-H(38,40), ^3J(H–H) = 7.0 Hz]; 8.47 [d, o-H(34,44), ^3J(H–H) = 7.0 Hz]; 8.42 [s, o'-H(22,32)]; 8.18 [d, o'-H(26,28), ^3J(H–H) = 7.2 Hz]; 7.76–7.90 (m, *meta* and *para* protons); 6.42 [d, S-H_5, ^3J(H–H) = 4.8 Hz]; 5.56 [t, S-H_4, ^3J(H–H) = 4.2 Hz]; 2.69 [d, S-H_3, ^3J(H–H) = 3 Hz]; 0.17 (s, OAc-Me), −1.42 (s, NH). ^{13}C NMR (150.87 MHz, 20 °C, $CDCl_3$): δ 154.0 [s, $C_\alpha(3,6)$]; 149.8 [s, $C_\alpha(13,16)$]; 152.2 (s) and 153.9 (s) for $C_\alpha(1,8)$ and $C_\alpha(11,18)$; 134.2 [s, $C_\beta(4,5)$]; 134.1 [s, $C_\beta(9,20)$]; 131.7 [s, $C_\beta(10,19)$]; 124.0 [s, $C_\beta(14,15)$]; 121.9 [s, C_m]; 155.5 [s, S-CO]; 131.4 [s, S-C_2]; 126.5 [s, S-C_3]; 126.0 [s, S-C_4]; 130.1 [s, S-C_5]; 176.6 [s, OAc-CO]; 18.9 [s, OAc-Me]. MS (FAB): $(M-OAc)^+$ 851 (calcd for $C_{49}H_{32}CdN_5OS$: 851). UV/Vis spectrum, λ (nm) [$\varepsilon \times 10^{-3}$ (M^{-1} cm^{-1})] in CH_2Cl_2: 432.9 (235.9), 543.0 (9.79), 584.0 (11.6), 639.0 (14.3).

2.5. NMR spectroscopy

Proton and ^{13}C NMR spectra were recorded at 599.95 and 150.87 MHz, respectively, on Varian Unity Inova-600 spectrometers locked on deuterated solvent, and referenced to the solvent peak. Proton NMR is relative to CD_2Cl_2 or $CDCl_3$ at $\delta = 5.30$ or 7.24 and ^{13}C NMR to the center line of CD_2Cl_2 or $CDCl_3$ at $\delta = 53.6$ or 77.0. The temperature of the spectrometer probe was calibrated by the shift difference of the methanol resonance in the ^1H NMR spectrum. HMQC (heteronuclear multiple quantum coherence) was used to correlate protons and carbon through one-bond coupling and HMBC (heteronuclear multiple bond coherence) for two- and three-bond proton–carbon coupling. Nuclear Overhauser effect (NOE) difference spectroscopy was employed to determine the ^1H–^1H proximity through space over a distance of up to about 4 Å.

The positive-ion fast atom bombardment mass spectrum (FAB-MS) was obtained in a nitrobenzyl alcohol (NBA) matrix using a JEOL JMS-SX/SX 102A mass spectrometer. UV/Vis spectra were recorded at 20 °C on a HITACHI U-3210 spectrophotometer.

2.6. X-ray crystallography

Table 1 presents the crystal data for **3** · $C_6H_5CH_3$ (*trans*) and **4** · CH_2Cl_2 (*cis*). Measurements were taken on a Bruker AXS SMART-1000 diffractometer using monochromatized Mo Kα radiation ($\lambda = 0.71073$ Å). Empirical absorption corrections were made for **3**-*trans* and **4**-*cis*. The structures were solved by direct methods (SHELXTL-97) [12] and refined by the full-matrix least-squares method. The furan group within **3**-*trans* is disordered with an occupancy factor of 0.6 for O(4)C(51) and 0.4 for O(4′)C(51′). These two atoms [i.e., O(4),C(51)] were refined with isotropic displacement parameters for **3**-*trans*. All non-hydrogen atoms except the above two atoms for **3**-*trans* were refined with anisotropic thermal parameters, whereas all hydrogen atoms were placed in calculated positions and refined with a riding model. Table 2 lists selected bond distances and angles for both **3** · $C_6H_5CH_3$ (*trans*) and **4** · CH_2Cl_2 (*cis*).

Table 1
Crystal structure data for **3** · $C_6H_5CH_3$ (*trans*) and **4** · CH_2Cl_2 (*cis*)

Empirical formula	$C_{58}H_{43}CdN_5O_4$ (**3** · $C_6H_5CH_3$ (*trans*))	$C_{52}H_{37}CdCl_2N_5O_3S$ (**4** · CH_2Cl_2 (*cis*))
Formula weight	986.37	995.23
Space group	$C2/c$	$P\bar{1}$
Crystal system	monoclinic	triclinic
a (Å)	26.0431(16)	8.6025(5)
b (Å)	11.1727(7)	10.2440(6)
c (Å)	31.847(2)	24.8640(13)
α (°)	90	90.616(1)
β (°)	91.995(2)	95.679(1)
γ (°)	90	97.452(1)
V (Å^3)	9260.9(10)	2161.3(2)
Z	8	2
F(000)	3984	1012
D_{calc} (g cm^{-3})	1.403	1.529
μ(Mo Kα) (mm^{-1})	0.527	0.730
S	1.004	1.045
Crystal size (mm)	0.31 × 0.10 × 0.02	0.30 × 0.10 × 0.10
θ (°)	28.35	28.31
T (K)	273(2)	100(2)
Number of reflections measured	11512	10677
Number of reflections observed	5680	8390 [$I > 2\sigma(I)$]
R_1[a]	0.0614	0.0551
wR_2[b]	0.1634	0.1321

[a] $R_1 = [\sum\|F_o\| - |F_c\|/\sum|F_o|]$.
[b] $wR_2 = \{\sum[w(F_o^2 - F_c^2)^2]/\sum[w(F_o^2)^2]\}^{1/2}$.

Table 2
Selected bond distances (Å) and angles (°) for compound **3** · $C_6H_5CH_3$ (*trans*) and **4** · CH_2Cl_2 (*cis*)

3 · $C_6H_5CH_3$ (*trans*)			
Bond lengths (Å)			
Cd(1)–N(1)	2.247(4)	Cd(1)–O(1)	2.302(4)
Cd(1)–N(2)	2.296(4)	Cd(1)–O(2)	2.325(4)
Cd(1)···N(3)	2.606(4)	Cd(1)···O(4)	5.098(4)
Cd(1)–N(4)	2.318(4)	Cd(1)···O(3)	5.144(4)
O(3)···O(4)	3.554(4)	O(4)···H(5A)	2.369(4)
Bond angles (°)			
O(1)–Cd(1)–O(2)	56.00(15)	O(2)–Cd(1)–N(1)	156.06(16)
O(1)–Cd(1)–N(1)	100.06(15)	O(2)–Cd(1)–N(2)	109.36(15)
O(1)–Cd(1)–N(2)	117.85(13)	O(2)–Cd(1)–N(4)	108.66(15)
O(1)–Cd(1)–N(4)	116.25(13)	N(2)–Cd(1)–N(4)	124.85(14)
N(1)–Cd(1)–N(2)	80.90(13)	O(4)···H(5A)–N(5)	104.35
N(1)–Cd(1)–N(4)	80.17(13)		
4 · CH_2Cl_2 (*cis*)			
Bond lengths (Å)			
Cd(1)–N(1)	2.277(3)	Cd(1)–O(1)	2.289(3)
Cd(1)–N(2)	2.278(3)	Cd(1)–O(2)	2.291(3)
Cd(1)–N(3)	2.303(3)	Cd(1)···O(3)	5.113(3)
Cd(1)···N(4)	2.617(3)	Cd(1)···S(1)	6.798(3)
O(3)···S(1)	2.991(3)		
Bond angles (°)			
O(1)–Cd(1)–O(2)	56.91(11)	O(2)–Cd(1)–N(1)	118.18(11)
O(1)–Cd(1)–N(1)	111.57(11)	O(2)–Cd(1)–N(2)	95.12(11)
O(1)–Cd(1)–N(2)	152.02(11)	O(2)–Cd(1)–N(3)	113.63(11)
O(1)–Cd(1)–N(3)	109.56(11)	N(1)–Cd(1)–N(3)	74.49(10)
N(1)–Cd(1)–N(2)	80.54(11)		
N(1)–Cd(1)–N(3)	125.59(10)		

3. Results and discussion

3.1. Molecular structures of 3 · $C_6H_5CH_3$ and 4 · CH_2Cl_2

Using a d^{10} metal, namely cadmium(II), the new complexes **3** · $C_6H_5CH_3$ and **4** · CH_2Cl_2 were synthesized. The synthetic strategy is outlined in Scheme 1. During the metallation of free bases **1** and **2** with $Cd(OAc)_2$ (Scheme 1), the soft acid Cd^{2+} prefers to retain one OAc^- ligand and coordinate to the N–H proton [i.e., H(2A)] of **1** and **2** to form six-coordinate complexes **3** and **4**. The molecular frameworks are depicted in Fig. 1a for **3** and in Fig. 1b for **4**.

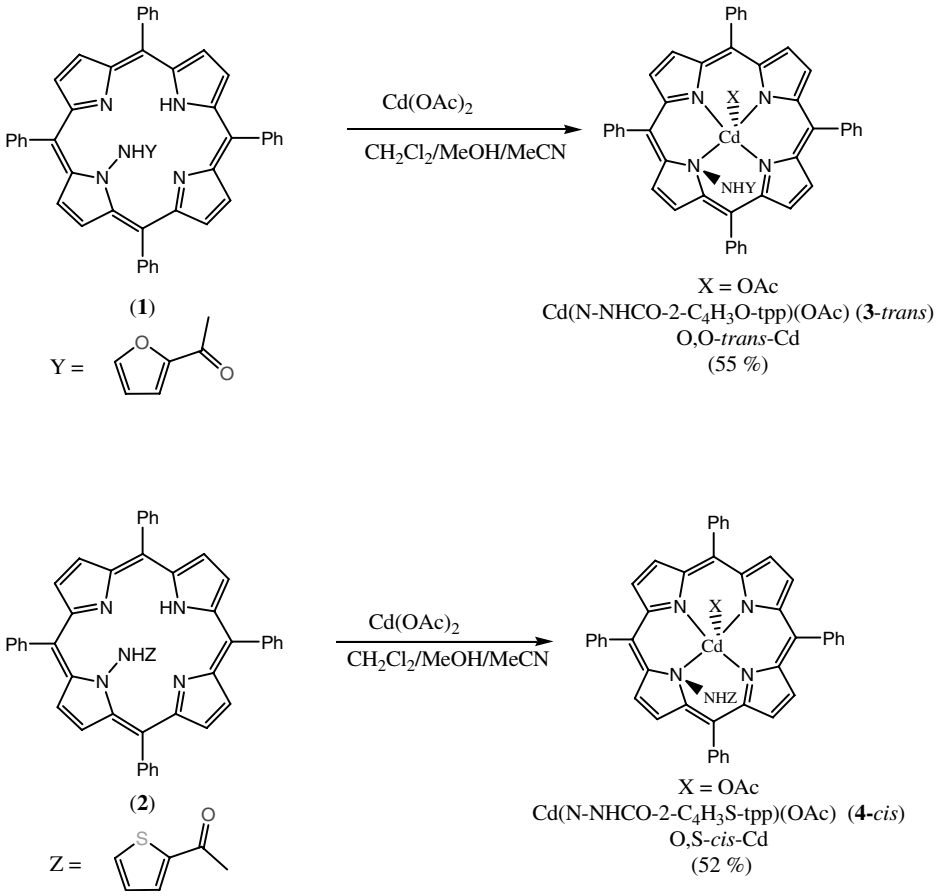

Scheme 1.

The bond distance (Å) of Cd(1)–O(1) is 2.302(4), Cd(1)–O(2) = 2.325(4), and the mean Cd(1)–N(p) = 2.287(4) Å for **3**; for **4**, the values are Cd(1)–O(1) = 2.289(3), Cd(1)–O(2) = 2.291(3) and the mean Cd(1)–N(p) = 2.286(3) Å (Table 2). The cadmium–nitrogen bond distances [Cd(1)–N(1) = 2.247(3), Cd(1)–N(2) = 2.296(4) and Cd(1)–N(4) = 2.318(4) Å of **3**; Cd(1)–N(1) = 2.277(3), Cd(1)–N(2) = 2.278(3) and Cd(1)–N(3) = 2.303(3) Å of **4**] are comparable to those of Cd(1)–N(p) = 2.301(5) Å in Cd(N–NHCO-C_6H_5-tpp)(OAc) [11]. The Cd(1)···N(3) distance of 2.606(4) Å for **3** [or Cd(1)···N(4) distance of 2.617(3) for **4**] is longer than 2.301(5) Å but is significantly shorter than the sum of the van der Waals radii of Cd and N (3.15 Å) [13]. This longer Cd···N(3) contact in **3** [or Cd···N(4) in **4**] may be viewed as a secondary intramolecular interaction. This kind of secondary interaction was earlier observed for both Cd(N-NHCOC_6H_5-tpp)(OAc) with Cd(1)···N(4) = 2.612(5) Å [11] and [Cd(H_3daps)Cl_4]$CH_3CN \cdot 0.25H_2O$ [H_4dap = 2,6-bis(1-salicyloylhydrazonoethyl)pyridine] with Cd···N(6) = 2.74(1) Å [14]. Most chemists seem to consider this secondary interaction between the metal ion and the fourth N as a weak bond in *N*-substituted porphyrin metal complexes. Furthermore, N(1), N(2) and N(4) [or N(1), N(2) and N(3)] are bonded strongly as well as covalently to the Cd atom in **3** [or **4**]. Thus the Cd(II)–2-furancarboxyamido-*meso*-tpp (**3**) and N-2-thiophenecarboxyamido-*meso*-tpp (**4**) structures are quite similar to metal(II) *N*-substituted porphyrin complexes with three strong and one weaker metal–N bond [11,15]. Compound **3** is an O,O-*trans* conformer in the solid phase with a dihedral angle of Ψ [O(3)–C(47)–C(48)–O(4)] = −174.17° and thus we are able to assign it as **3**-*trans*. Compound **4** is an O,S-*cis* conformation (i.e., **4**-*cis*) in the solid phase with Ψ [O(3)–C(47)–C(48)–S(1)] = 1.59°. The geometry around Cd^{2+} is described as a distorted square-based pyramid in which the apical site is occupied by a bidentate chelating OAc^- group in **3**-*trans* and **4**-*cis*. Fig. 2 shows the actual porphyrin skeleton of **3**-*trans* and **4**-*cis*.

We adopt the plane of three strongly bound pyrrole nitrogen atoms [i.e., N(1), N(2) and N(4) for **3**-*trans* and N(1), N(2) and N(3) for **4**-*cis*] as a reference plane, 3N. In **3**-*trans* (or **4**-*cis*), Cd^{2+} and N(5) are located on different sides at 1.06 (or 1.04) and −1.49 Å (or −1.53 Å) from its 3N plane, respectively (Fig. 2). The N(3) and N(4) pyrrole rings bearing the 2-furancarboxamido (Fr) and 2-thiophenecarboxamido groups in **3**-*trans* and **4**-*cis*, respectively, deviate mostly from the 3N plane, thus orienting separately with a dihedral angle of 33.4° and of 31.0°, whereas small angles of 0.7°, 18.5° and 23.7° occur with N(1), N(4) and N(2) pyrrole for **3**-*trans*

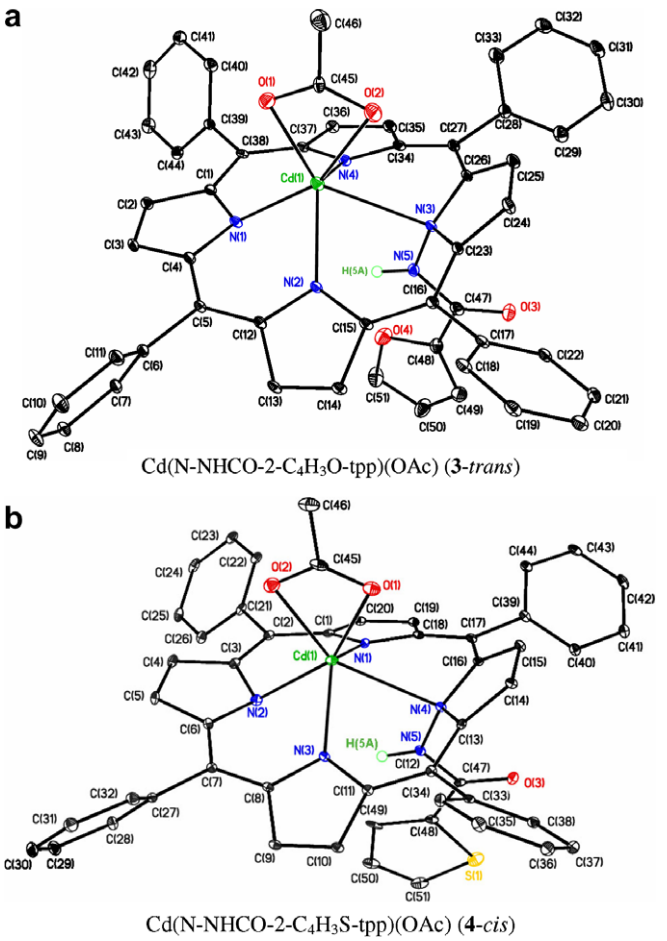

Fig. 1. Molecular configuration and atom-labelling scheme for (a) $\mathbf{3}\cdot C_6H_5CH_3$ (*trans*) and (b) $\mathbf{4}\cdot CH_2Cl_2$ (*cis*), with ellipsoids drawn at 30% probability. Hydrogen atoms, solvent $C_6H_5CH_3$ for $\mathbf{3}\cdot C_6H_5CH_3$ (*trans*) and CH_2Cl_2 for $\mathbf{4}\cdot CH_2Cl_2$ (*cis*) are omitted for clarity.

and the corresponding angles are 18.2°, 23.5° and 17.6° with N(2), N(1) and N(3) pyrrole for **4**-*cis*. In **4**-*cis*, such a large deviation from planarity for the N(4) pyrrole is also reflected by observing a 7.7–10.2 ppm upfield shift of the C_β(C14, C15) at 124.0 ppm compared to 131.7 ppm for C_β(C10, C19), 134.1 ppm for C_β(C9, C20) and 134.2 ppm for C_β(C4, C5). In **3**-*trans*, a similar deviation is also found for N(3) pyrrole by observing a 7.6–10.2 ppm upfield shift of C_β(C24, C25) at 123.9 ppm compared to 134.11 ppm for C_β(C2, C3), 134.06 ppm for C_β(C13, C36) and 131.5 ppm for C_β(C14, C35).

It is noted that the ionic radius for the metal ion increases from 0.82 Å for Zn^{2+} with a coordination number (CN = 5) to 1.09 Å for Cd^{2+} (CN = 6). Because of the larger size of Cd^{2+}, Cd(1), O(2) and O(1) lie 1.06, 2.88 and 3.24 Å, respectively, above the 3N plane in **3**-*trans*, compared to 1.04 Å for Cd(1), 2.92 Å for O(1) and 3.16 Å for O(2) in **4**-*cis* [cf. 0.65 Å for Zn^{2+} in Zn(N-Me-tpp)Cl] (Fig. 2) [16].

The dihedral angles between the mean plane of the skeleton (3N) and the planes of the phenyl groups are 57.6° [C(9)], 32.1° [C(20)], 32° [C(31)] and 56.4° [C(42)] for

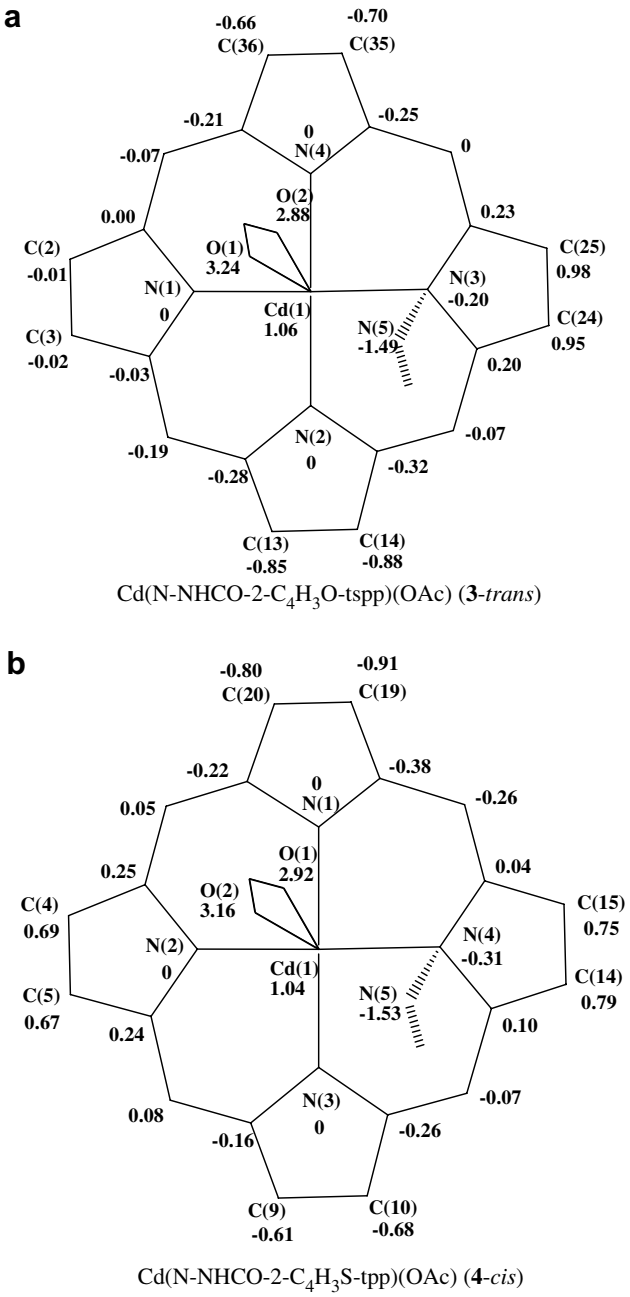

Fig. 2. Diagram of the porphyrinato core ($C_{20}N_4$, Cd, furan, thiophene and OAc) of (a) **3**-*trans* and (b) **4**-*cis*. The values represent the displacement (in Å) of the atoms from the 3N plane [i.e., N(1), N(2), N(4) for **3**-*trans* and N(1)–N(3) for **4**-*cis*].

3-*trans* and the corresponding angles are 44.7°, 42.9°, 34.3° and 35.7° for **4**-*cis*.

3.2. ^1H and ^{13}C NMR spectroscopy data of 3-trans and 4-cis in $CDCl_3$

The singlet at −0.35 ppm was assigned to NH protons [i.e., H(2A) and H(5A)] for **2** at 20 °C. Moreover, the signal arising from the NH protons [i.e., H(2A) and H(5A)] of **1** was not observed at 20 °C. At −90 °C, traces of water were

frozen from solution of **1** in CD_2Cl_2. Thus, the frozen water inhibits intermolecular proton exchange between water and NH protons of **1** and allows the observation of a broad singlet for the NH proton at −0.61 ppm ($\Delta\nu_{1/2} = 23$ Hz). Upon metallation, there were no signal of NH (in pyrrole) [i.e., H(1A) for **3** and H(2A) for **4**] for metal porphyrins **3** and **4**. The ^{1}H NMR spectrum of **3** (or **4**) in $CDCl_3$ (Figs. 3 and 4) showed a sharp singlet at $\delta = -0.99$ (or −1.23) ppm ($\Delta\nu_{1/2} = 4$ Hz) for the NH proton at 20 °C. These NMR data for **3** (or **4**) suggest that the NH proton [i.e., H(5A)] bound to N(5) undergoes rapid intermolecular proton exchange with water at 20 °C.

Complexes **3**-*trans* and **4**-*cis* were characterized by ^{1}H (Figs. 3 and 4) and ^{13}C NMR spectra. In solution, the molecule has effective C_s symmetry with a mirror plane running through the N(5)–N(3)–Cd(1)–N(1)–O(1)–O(2) unit for **3**-*trans* or the N(5)–N(4)–Cd(1)–N(2)–O(1)–O(2) unit for **4**-*cis* (Fig. 1). There are four β-pyrrole protons H_β, four β-pyrrole carbons C_β, four α-pyrrole carbons C_α, two different *meso* carbons C_{meso} and two phenyl-C_1 carbons for these two complexes. In **4**-*cis*, the doublet at 8.76 ppm is assigned to $H_\beta(10,19)$ with $^3J(H–H) = 4.2$ Hz, and the other doublet at 8.72 ppm with $^3J(H–H) = 4.2$ Hz is due to $H_\beta(9,20)$ (Fig. 3a). The singlet at 8.89 ppm is assigned to $H_\beta(4,5)$ and the other singlet at 8.63 ppm is due to $H_\beta(14,15)$ (Fig. 3a). In **3**-*trans*, the doublet at 8.76 ppm is due to $H_\beta(14,35)$ with $^3J(H–H) = 4.5$ Hz and the other doublet at 8.73 ppm is due to $H_\beta(13,36)$ with $^3J(H–H) = 4.5$ Hz (Fig. 4a). The singlet at 8.89 ppm is assigned to $H_\beta(2,3)$ and the other singlet at 8.61 ppm is due to $H_\beta(24,25)$ (Fig. 4a).

Fig. 3 depicts the representative ^{1}H spectra for **4**-*cis* in $CDCl_3$ at 20 and −50 °C. At 20 °C, the rotation of the phenyl group along C_1–C_{meso} [C(17)–C(39) or C(12)–C(33)]

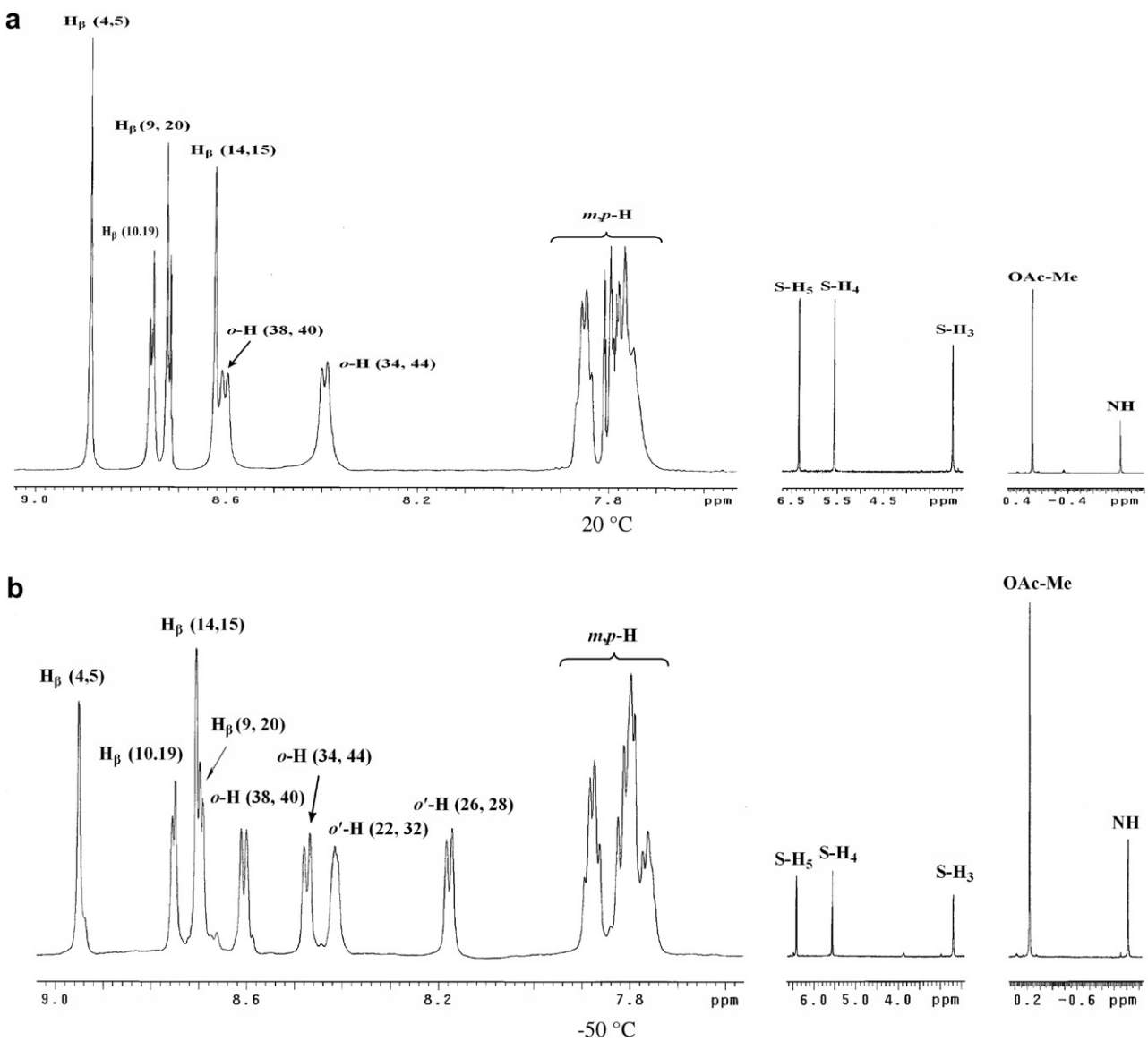

Fig. 3. ^{1}H NMR spectra for **4**-*cis* at 599.95 MHz in $CDCl_3$: (a) 20 °C, (b) −50 °C, where S = 2-thiophenecarboxamido.

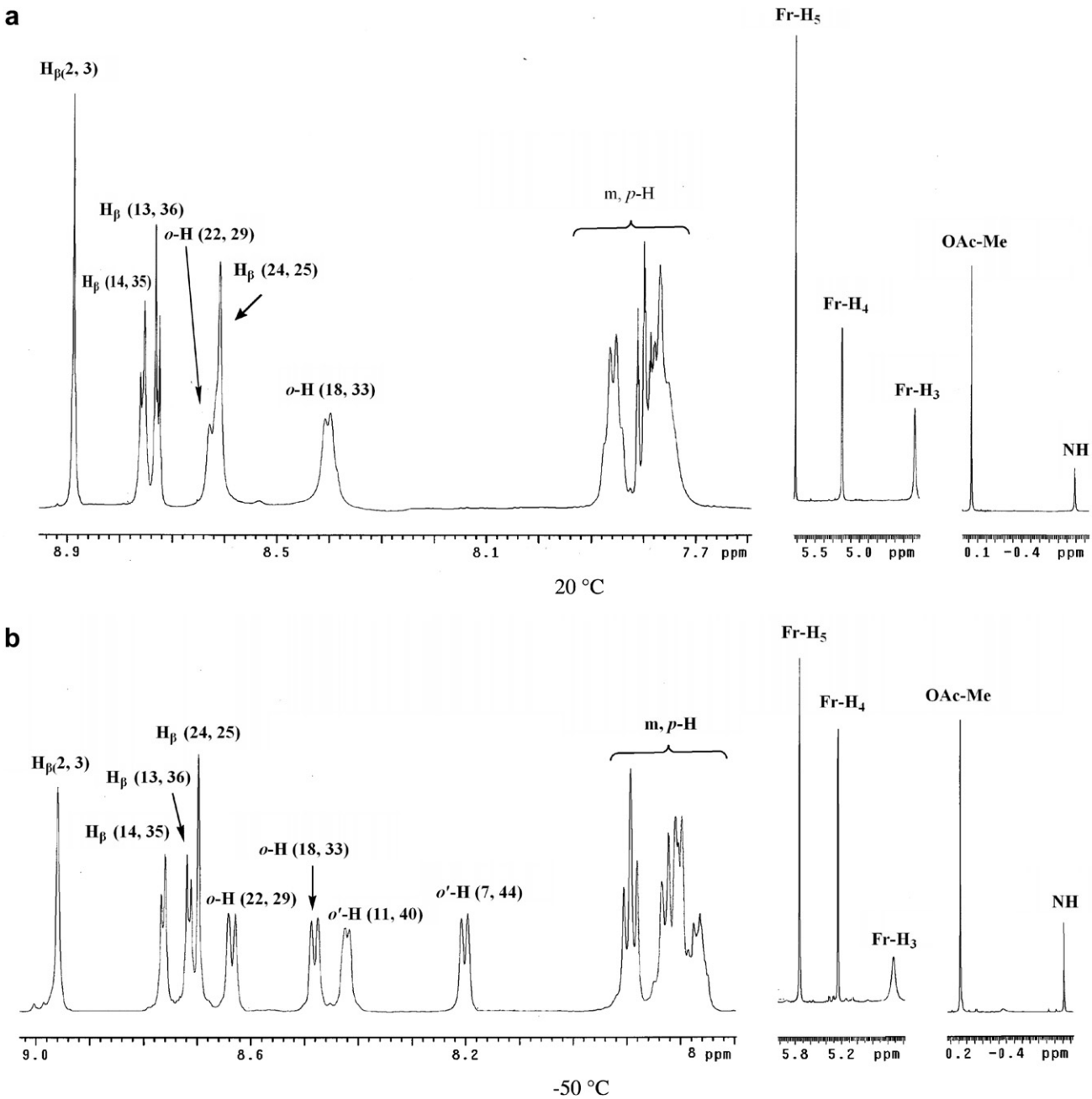

Fig. 4. ^{1}H NMR spectra for **3**-*trans* at 599.95 MHz in $CDCl_3$: (a) 20 °C, (b) −50 °C, where Fr = 2-furancarboxamido.

bond is slow. This slow rotation is supported by the two singlets at 8.60 and 8.40 ppm due to *o*-H(38,40) and *o*-H(34,44), respectively (Fig. 3a). Moreover, the rotation of the phenyl group along C(7)–C(27) [or C(2)–C(21)] bond for **4**-*cis* is at the intermediate exchange region. In this intermediate exchange region, the signals are broadened beyond detection. Hence, no signals of *o*′-H(22,32) and *o*′-H(26,28) for **4**-*cis* have been observed at 20 °C (Fig. 3a). At −50 °C, this rotation is extremely slow. Hence, the rate of intramolecular exchange of the *ortho* protons for **4**-*cis* in $CDCl_3$ is also extremely slow. The doublet at 8.61 ppm is assigned to *ortho* protons *o*-H(38,40) with ^3J(H–H) = 7.0 Hz (Fig. 3b). The other doublet at 8.47 ppm is due to *ortho* protons *o*-H(34,44) with ^3J(H–H) = 7.0 Hz. Likewise, the singlet at 8.42 ppm is due to *ortho* proton *o*-H(22,32). The corresponding doublet at 8.18 ppm is due to *o*-H(26,28) with ^3J(H–H) = 7.2 Hz (Fig. 3b). The interpretation of these data were confirmed by the NOE difference spectroscopy for **4**-*cis* in $CDCl_3$ at 20 and −50 °C.

In a similar fashion, the rotation for the phenyl group of **3**-*trans* in $CDCl_3$ at 20 °C along C(27)–C(28) [or C(16)–C(17)] bond is slow and the rotation along C(38)–C(39) [or C(5)–C(6)] is at the intermediate exchange region. Hence, the ^{1}H resonances for the *ortho* protons of **3**-*trans* were observed as two sets of doublets: one doublet at 8.62 ppm is assigned to *ortho* protons *o*-H(22,29) with

Table 3
Group net charges (q) for **3** and **4** by NBO calculations[a]

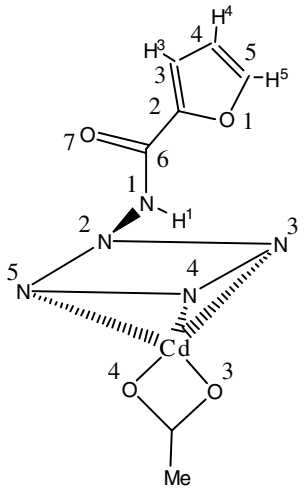

3-*trans*

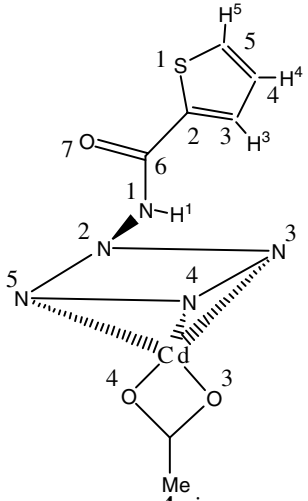

4-*cis*

Compound	Conformer	Metal	O^1	S^1	C^2	C^3	C^4	C^5	C^6	O^7	N^1	N^2	N^3	N^4	N^5	O^3	O^4
O,O-Cd	**3**-*trans*	1.674	−0.473		0.227	−0.201	−0.269	0.188	0.635	−0.626	−0.399	−0.324	−0.739	−0.721	−0.727	−0.832	−0.799
O,S-Cd	**4**-*cis*	1.676		0.490	−0.310	−0.168	−0.202	−0.355	0.661	−0.634	−0.415	−0.317	−0.733	−0.719	−0.747	−0.834	−0.803

[a] Group net charges including the attached hydrogen by NBO* calculations.
*E.D. Glendening, A.E. Reed, J.E. Carpenter, F. Weinhold, NBO Version 3.1 in GAUSSIAN-03.

^3J(H–H) = 6.6 Hz and the other doublet at 8.40 ppm is due to *ortho* protons *o*-H(18,33) with ^3J(H–H) = 6.6 Hz (Fig. 4a). Moreover, no signals of *o′*-H(11,40) and *o′*-H(7,44) of **3**-*trans* have been detected at 20 °C (Fig. 4a). However, for *ortho* protons, at −50 °C, the rotation of phenyl group along the C_1–C_{meso} bond in **3**-*trans* is extremely slow, which is evident from the appearance of the four doublets at 8.64 [*o*-H(22,29)], 8.48 [*o*-H(18,33)], 8.42 [*o′*-H(11,40)], and 8.20 [*o′*-H(7,44)] ppm due to four different *ortho* protons of the aromatic ring (Fig. 4b).

Due to the ring current effect, upfield shifts for the ^{1}H resonances of S-H_5, S-H_4 and S-H_3 for **4** with the O,S-*cis* conformer in $CDCl_3$ at −50 °C are $\Delta\delta = -1.21$ [from 7.63 (obtained from 2-acetylthiophene) to 6.42 ppm], −2.13 (from 7.69 to 5.56 ppm) and −4.44 ppm (from 7.13 to 2.69 ppm), respectively (Fig. 3b). Qualitatively, as the distance between the geometrical center (C_t) of the 4N plane and axial protons gets smaller, the shielding effect becomes larger. In **4**-*cis*, the distance for $C_t\cdots$S-H_3, $C_t\cdots$S-H_4 and $C_t\cdots$S-H_5 increases from 3.235, 5.738 to 7.066 Å, individually. As the S-H_3 proton of **4**-*cis* is closer to C_t, the shielding gets larger for this S-H_3. A similar ring current effect is also observed for **3**-*trans*. The occurrence of weak intramolecular hydrogen bonding between one amino hydrogen [H(5A)] and the furan oxygen [O(4)] in O,O-*trans* of **3** is reflected in the long N(5)–H(5A)···O(4) (furan) bond distance of 2.358 Å and acute N(5)–H(5A)···O(4) (furan) angle of 104.35° (Fig. 1a) [6]. The hydrogen bonding results in a downfield shift of 0.24 ppm for the NH proton which resonances from −1.23 ppm for **4**-*cis* (O,S-*cis*-Cd) to −0.99 ppm for **3**-*trans* (O,O-*trans*-Cd) in $CDCl_3$ at 20 °C (Figs. 3 and 4). This intramolecular H-bonding and electrostatic attraction between $Cd(1)^{2+}$ and $O(4)^-$ restricts the rotation of the furan group along the C(48)–C(47) bond. Thus, as the temperature is increased from −50 °C to 20 °C for **3**-*trans* in $CDCl_3$, Fr-H_3 rotates a degree slightly closer to C_t and a minimum upfield shift of −0.15 ppm was observed for the ^{1}H resonances of Fr-H_3 from 4.52 to 4.37 ppm (Fig. 4).

X-ray diffraction analysis unambiguously confirms that **3**-*trans* and **4**-*cis* have a chelating bidentate OAc^- ligand in the solid phase. Notably, the ring current effects seldom exceed 10 ppm in ^{1}H NMR [17] and 2 ppm in ^{13}C NMR [18]. Hence, the ring current contribution is relatively less important in determining the ^{13}C chemical shifts than proton shifts. The ^{13}C NMR chemical shifts were shown to be a useful tool for diagnosing the nature of acetate ligands, whether unidentate or bidentate in diamagnetic complexes. Unidentate acetate ligands were located at 20.5 ± 0.2 and 168.2 ± 1.7 ppm and bidentate acetate ligands at 18.0 ± 0.7 and 175.2 ± 1.6 ppm [17]. The methyl and carbonyl chemical shifts of the acetate group in **3**-*trans* (or **4**-*cis*) at 20 °C in $CDCl_3$ are separately located at 18.9 (or 18.9) and 176.3 (or 176.6) ppm confirming that the acetate is chelating bidentately and is coordinated to the cadmium atom in **3**-*trans* (or **4**-*cis*) in the solution phase. The difference in chemical shifts for the CO group to be characteristic of either uni- or bidentate acetates are definitely out of the range of the shielding effect of a porphyrin.

NBO group net charges over O(4), O(3) and Cd(1) in **3** (O,O-*trans*-Cd; **3**-*trans*) are −0.473, −0.626 and 1.674, respectively (Table 3). In **3**-*trans*, a weakly repulsive electrostatic interaction between the two oxygen atoms [i,e., $O(3)^-$ and $O(4)^-$] and a strongly attractive electrostatic force between the cadmium [$Cd(1)^{2+}$] and oxygen atom [$O(4)^-$] are two major factors explaining the *trans* conformer of **3** which dominates both in the solid phase and in low polar solvents at low temperature. Group charges for S(1), O(3) and Cd(1) in **4** (O,S-*cis*-Cd; **4**-*cis*) are 0.490, −0.634 and 1.676, respectively (Table 3). In **4**-*cis*, a moderately electrostatic attraction between the sulfur [$S(1)^+$] and oxygen atom [$O(3)^-$] and weakly repulsive electrostatic force between the cadmium [$Cd(1)^{2+}$] and sulfur [$S(1)^+$] are two major factors determining that the *cis* conformer of **4** is favored both in the solid and in low polarity solvents at low temperature.

4. Conclusion

We have investigated two new, diamagnetic and mononuclear cadmium(II) *N*-substituted-*N*-aminoporphyrin complexes **3**-*trans* and **4**-*cis* which exist in O,O-*trans* and O,S-*cis* conformers, respectively, and their X-ray structures have been established. We also demonstrate how the electrostatic repulsive and attractive forces influence the favorable conformers in the case of **3**-*trans* and **4**-*cis*. Both the electrostatic attraction between Cd^{2+} and $O(4)^-$ and the N–H···O (furan) H-bond interaction stabilized the O,O-*trans* form of **3**-*trans* in $CDCl_3$ at −50 °C. Both the electrostatic repulsion between Cd^{2+} and $S(1)^+$ and the attractive interaction between $S(1)^+$ and $O(3)^-$ stabilize the O,S-*cis* conformer of **4**.

Acknowledgment

Financial support from the National Science Councils of the ROC under Grant NSC 94-2113-M-005-010 is gratefully acknowledged.

Appendix A. Supplementary material

Fig. S1 shows the molecular structure for O,O-*cis* of **1** at 100(2) K. Fig. S2 shows the molecular structures for O,S-*cis* and O,S-*trans* of **2** at 100(2) K. CCDC 289590 and 289591 contains the supplementary crystallographic data for **3** and **4**. These data can be obtained free of charge via http://www.ccdc.cam.ac.uk/conts/retrieving.html, or from the Cambridge Crystallographic Data Centre, 12 Union Road, Cambridge CB2 1EZ, UK; fax: (+44) 1223-336-033; or e-mail: deposit@ccdc.cam.ac.uk. Supplementary data associated with this article can be found, in the online version, at doi:10.1016/j.poly.2006.08.034.

References

[1] I.S. Han, C.K. Kim, H.J. Jung, I. Lee, Theor. Chim. Acta 93 (1996) 199.
[2] R. Benassi, U. Folli, L. Schenetti, F. Taddei, J. Chem. Soc., Perkin Trans. II (1987) 961.
[3] S.R. Salman, Org. Magn. Reson. 20 (1982) 151.
[4] L. Lunazzi, G. Placucci, C. Chatgilialoglu, D. Macciantelli, J. Chem. Soc., Perkin Trans. II (1984) 819.
[5] D. Casarini, L. Lunazzi, D. Macciantelli, J. Chem. Soc., Perkin Trans. II (1985) 1839.
[6] R. Crespo-Otero, L.A. Montero, G. Rosquete, J.A. Padron-Garcia, R.H. Gonzalez-Jonte, J. Comput. Chem. 25 (2004) 429.
[7] H.J. Callot, Tetrahedron 35 (1979) 1455.
[8] H.J. Callot, J. Fischer, R. Weiss, J. Am. Chem. Soc. 104 (1982) 1272.
[9] H.J. Callot, B. Chevrier, R. Weiss, J. Am. Chem. Soc. 100 (1978) 4733.
[10] K. Ichimura, Bull. Chem. Soc. Jpn. 51 (1978) 1444.
[11] F.A. Yang, J.H. Chen, H.Y. Hsieh, S. Elango, L.P. Hwang, Inorg. Chem. 42 (2003) 4603.
[12] G.M. Sheldrick, SHELXL-97: Program for the Refinement of Crystal Structures from Diffraction Data, University of Göttingen, Göttingen, Germany, 1997.
[13] R.D. Shannon, Acta Crystallogr., Sect. A 32 (1976) 751.
[14] M. Fundo, A. Sousa, M.R. Bermejo, A. Gaorcia-Deibe, A. Sousa-Pedrares, O.L. Hoyos, M. Helliawall, Eur. J. Inorg. Chem. (2002) 703.
[15] M. Ravikanth, T.K. Chandrashekar, Struct. Bond. 82 (1995) 105.
[16] D.K. Lavellee, A.B. Kopelove, O.P. Anderson, J. Am. Chem. Soc. 100 (1978) 3025.
[17] S.J. Lin, T.N. Hong, J.Y. Tung, J.H. Chen, Inorg. Chem. 36 (1997) 3886.
[18] E. Breitmaier, W. Voelter, Carbon-13 NMR Spectroscopy, 3rd ed., VCH, New York, 1990, pp. 110, 116, 117.